

# Simulations of Cell-Surface Integrin Binding to Nanoscale-Clustered Adhesion Ligands

Darrell J. Irvine, Kerri-Ann Hue, Anne M. Mayes, and Linda G. Griffith\*

Department of Materials Science and Engineering, Department of Chemical Engineering, and the Division of Bioengineering and Environmental Health, Massachusetts Institute of Technology, Cambridge, Massachusetts 02139 USA

**ABSTRACT** Clustering of ligated integrins strongly influences integrin signaling and mechanical linkages between integrins and intracellular structures. Extracellular spatial organization of integrin ligands in clusters may facilitate clustering of bound integrins and thus potentially regulate cellular responses to a defined average amount of ligand in the extracellular environment. The possible role of such ligand clustering effects in controlling overall receptor occupancy is studied here using a simple mass-action equilibrium model as well as a two-dimensional Monte Carlo lattice description of the cell-substrate interface, where cell surface receptors are free to diffuse in the plane of the interface and interact with the substrate-immobilized ligand. Results from the analytical treatment and simulation data indicate that for a single-state model in which receptor-ligand binding equilibria are not influenced by neighboring complexes, clustering of ligand does not enhance total receptor binding. However, if receptor binding energy increases in the presence of neighboring ligated receptors, strong ligand spatial distribution effects arise. Nonlinear responses to increasing ligand density are also observed even in the case of random ligand placement due to stochastic juxtaposition of ligand molecules. These results describe how spatial distribution of ligand presented by the extracellular matrix or by synthetic biomimetic materials might control cell responses to external ligands, and suggest a feedback mechanism by which focal contact formation might be initiated.

## INTRODUCTION

Cell adhesion to extracellular matrices (ECMs), basement membranes, other cells, and artificial biomimetic matrices, i.e., to (approximately) fixed physical structures in the extracellular environment, is governed by a diverse array of adhesion receptors that bind to extracellular ligands and initiate biochemical signaling pathways similar to growth factor receptors (Aplin et al., 1998; Hynes 1999). A common feature of adhesion receptors is their propensity to cluster or aggregate when bound to ligand. This clustering is typically associated with recruitment of cytosolic proteins to form intracellular macromolecular complexes that link the receptors to the cytoskeleton, to signaling pathways, or to both (Aplin et al., 1998). These linkages, in turn, influence cell survival, growth, differentiation, and migration.

Adhesion receptor clustering appears to play a key role in physiological cell responses to adhesion ligands (Hato et al., 1998; Kornberg et al., 1991; LaFlamme et al., 1992; Lotz et al., 1989; Maheshwari et al., 2000; Miyamoto et al., 1995a,b, 1996; Oh et al., 1997; Yauch et al., 1997). A physiological role for clustering has been particularly well established for integrins, the major family of adhesion receptors for ECM molecules such as fibronectin, collagen, vitronectin, and laminin. Integrin aggregation strongly influences both the biochemical and biomechanical functions

of the receptors, in part via the hierarchy of cytosolic proteins recruited to sites of integrin aggregation. These molecules assemble into the macroscopic structures with sizes as large as 0.1–1  $\mu\text{m}$  diameter with variable intracellular molecular composition and morphologies ranging from spot-like to fibrillar (Adams, 2001; Burridge and Chrzanowska-Wodnicka, 1996; Segel et al., 1983; Zamir et al., 1999). Integrin aggregation has been almost exclusively studied in cell culture, leading to speculation that the structures formed may not be representative of in vivo cell behavior. New experimental approaches based on green fluorescent protein tags have revealed not only the presence of aggregates in migrating cells in vivo, but also their dynamic nature (Knight et al., 2000).

Both occupancy and clustering seem essential to elicit the full range of cellular responses mediated by integrins. Integrins show an enhanced propensity to cluster and interact with the cytoskeleton upon ligand binding (LaFlamme et al., 1992; Yauch et al., 1997). Mutations in the cytoplasmic domain of integrins that impair integrin diffusion and clustering also impair cell adhesion and spreading (Yauch et al., 1997). Although integrins have no intrinsic enzymatic activity in their cytoplasmic tails, they serve as signaling centers through the accessory molecules of focal contacts (Clark and Brugge, 1995). Both integrin ligation and clustering are required for integrin-mediated signaling (Kornberg et al., 1991) and for engaging interactions with a full complement of both cytoskeletal and signaling proteins (Miyamoto et al., 1995a,b, 1996). The formation of focal adhesions, indicative of large integrin aggregates, enhances the adhesion strength of cells to matrix during the initial attachment period (Lotz et al., 1989) and in longer-term culture (Maheshwari et al., 2000). Similarly, disassembly of

---

Received for publication 5 October 2000 and in final form 11 November 2001.

Address reprint requests to Dr. Linda G. Griffith, MIT 66–466, 77 Massachusetts Avenue, Cambridge, MA 02139. Tel.: 617-253-0013; Fax: 617-258-5042; E-mail: griff@mit.edu

© 2002 by the Biophysical Society

0006-3495/02/01/120/13 \$2.00

focal adhesions via growth factor addition is associated with reduced cell adhesion (Xie et al., 1998).

Formation and turnover of integrin aggregates or focal adhesions plays a role in many aspects of cell behavior. For example, formation and release of focal adhesions is required for cell migration (Lauffenburger and Horwitz 1996). Increased turnover of focal adhesions is associated with greater cell migration speeds *in vitro* on flexible versus rigid substrata (Pelham and Wang 1997). The process of integrin aggregation and focal contact formation requires both a sufficiently high local ligand density in the extracellular environment as well as multivalent talin complexes for intracellular cross-linking of integrins to each other via their cytoplasmic tails (Ward and Hammer 1994). A quantitative model of how receptor aggregation is influenced by the relative contributions of receptor-ligand, receptor-cytoskeleton, and cytoskeleton-cytoskeleton interactions in the presence of uniform densities of extracellular integrin ligands has shown that the aggregation process is especially sensitive to the self-association constant of cytoskeletal proteins, a parameter that might change in value upon biochemical activation of receptors (Ward and Hammer 1994).

We speculate further that spatial organization of ligand into discrete clusters of locally high ligand density may enable more efficient integrin aggregation. Physiological ligand clustering can be inferred from the structure of matrix molecules and of assembled ECM *in vitro* and *in vivo*. Many ECM proteins are multimeric, with many sites for adhesion receptor binding located within the same molecule (Chothia and Jones 1997; Hynes and Yamada, 1982; Nomizu et al., 1998). For example, tenascin-C is a hexameric molecule comprising two triplets of arms joined to form a hexabrachion structure (Aukhil et al., 1993; Spring et al., 1989). In electron micrographs, each arm is  $\sim 100$  nm in length and has a globular domain, identified as the cell-binding region, distal to the center of the hexabrachion (Spring et al., 1989). Thus, tenascin-C effectively presents a nanocluster of six adhesion sites. Multimeric molecules may also be organized into supramolecular structures presenting discrete adhesion domains within the extracellular environment. In connective tissue such as dermis, collagen I fibers form randomly arrayed fibrillar bundles ranging from 100 to 1000 nm in diameter (Friedl and Bröcker, 2000a). Cells form discrete adhesions to these bundles in a manner that has been described as a process of ligand-induced receptor clustering (Friedl and Bröcker, 2000a). Fibronectin is actively organized by cells into polymerized networks, to which cells show organized adhesion (Hynes and Yamada, 1982). Loss of fibronectin matrix organization is observed in patients with Ehlers-Danlos syndrome and is associated with severely impaired wound healing; restoration of normal wound healing, accomplished by treating patients with dexamethasone, is accompanied by restoration of normal fibronectin matrix organization (de Panfilis et al., 2000).

Experimental evidence that ligand clustering influences integrin-mediated cell behavior comes from recent development of methods to present single peptide adhesion ligands in a nano-clustered manner, i.e., where the average ligand density, cluster size, and average cluster spacing can be independently controlled (Banerjee et al., 2000; Danilov and Juliano, 1989; Irvine et al., 2001; Maheshwari et al., 2000). This approach has revealed that both the size and average density of integrin ligand clusters strongly control cell adhesion and migration in response to an RGD adhesion ligand and that randomly presented ligand was ineffective in eliciting migration (Maheshwari et al., 2000).

A theoretical understanding of how integrin clustering is controlled by the spatial distribution of extracellular ligand is intrinsically relevant to understanding integrin physiology, and of great practical importance for guiding the design of new biomaterials. The present work was undertaken to theoretically predict patterns of receptor binding to spatially inhomogeneous ligand distributions on a surface. A simple analytical model and lattice Monte Carlo simulations were used to study how integrin clustering might be induced at the interface between a cell membrane and a substrate via ligand immobilized in small, randomly distributed clusters on the substrate. Presenting ligand in high-density clusters forces some *de facto* clustering of receptors due to normal receptor-ligand equilibria.

We first investigated whether such clustering could play a role in focal adhesion development by increasing the total number of receptor-ligand bonds compared with a uniform distribution at equal total ligand concentration. Second, we explored how increases in effective receptor-ligand affinity caused by receptor clustering might escalate local ligand binding, further driving focal contact formation and strengthening cell-substrate adhesion in the presence of clustered ligand distribution. In this regard, our model builds on a previous analytical model that showed how cooperativity effects could give rise to patchy adhesion domains in the presence of uniformly distributed ligand for certain combinations of receptor-ligand on/off rates and receptor diffusion coefficients (Segel et al., 1983). Here, changes in the effective receptor-ligand affinity were modeled using a two-state binding energy: discrete receptor-ligand bonds have an energy  $E_1$ , whereas complexes forming next to existing receptor-ligand pairs have a second energy  $E_2$ , where  $|E_2| > |E_1|$ . We examined under what conditions (ligand distributions, local and average surface densities, and receptor-ligand binding energies) ligands presented in clusters can modify the number of receptor-ligand bonds formed at the cell-substrate interface, an important factor in cell response. Simulations predict that for modest increases of the effective binding affinity on clustering, for even very small cluster sizes ( $2 \times 2$  or  $3 \times 3$  ligand arrays), the number of total bonds formed at equilibrium can be increased by a factor of 2–20 by clustering ligand over a broad range of total ligand densities.

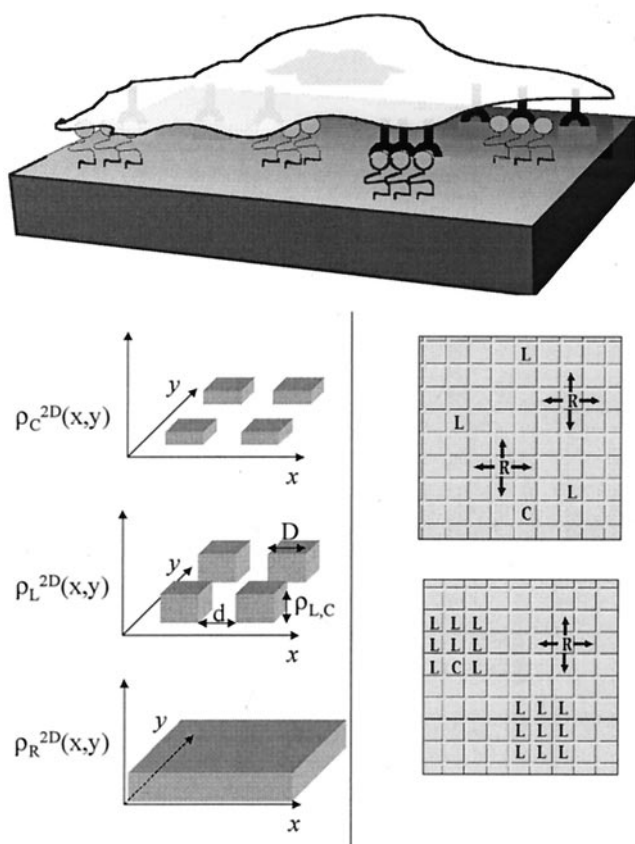


FIGURE 1 Schematics of models for the cell membrane-substrate interface. (Top) Schematic of the physical situation modeled. (Bottom left) Two-dimensional representation of a clustered ligand substrate-cell membrane interface. Initial receptor concentration within the plasma membrane is uniform, but the ligand distribution (and thus the complex distribution) at the surface is spatially variant. (Bottom right) Monte Carlo model. The interface of a cell membrane juxtaposed with a surface presenting tethered ligands is modeled as a two-dimensional square lattice. Each site of the lattice may be occupied by a tethered ligand (L), mobile receptor (R), or tethered receptor-ligand complex (C). Clustered ligand surfaces are modeled by placing ligands in ordered arrays; the clusters are distributed randomly on the 2D lattice.

## DESCRIPTION OF THE CELL-SUBSTRATE INTERFACE

An analytical model and a Monte Carlo simulation were developed to model the interface between a cell membrane and a rigid substrate. The models consider the interaction of cell integrin receptors with ligand immobilized on the substrate discretely (i.e., randomly) or in clusters (groups of ligand confined to a defined area). The physical picture is schematically shown in Fig. 1. The cell membrane is flat against the substrate with a constant separation of  $300 \times 10^{-8}$  cm, comparable to the distance over which integrins can interact with ligand (Lauffenburger and Linderman, 1993). Several studies have shown that unligated integrins are freely diffusible in the plane of the membrane, especially at the leading edges of migrating cells and at the cell

periphery where new adhesions form (Duband et al., 1988; Schmidt et al., 1993; Yauch et al., 1997). We thus neglect interactions between integrins and other membrane components. Ligand is immobilized on the surface, modeling the case of strongly adsorbed adhesion proteins or, as depicted in Fig. 1, peptide ligand bound to an artificial substrate via short tethers.

## Two-dimensional analytical model for one-state binding

The effect of ligand surface distribution on equilibrium receptor binding was first analyzed for the case when the receptor-ligand binding energy is not affected by nearest-neighbor interactions between receptors; i.e., only one state exists for bound receptors. This situation is amenable to an analytical model and provides an initial physical insight for comparison with the two-dimensional, two-state Monte Carlo simulation described in the next section. A two-dimensional (2D) strip of the 2D cell-substrate interface is considered. It is assumed for simplicity in this calculation that the ligand clusters are regularly distributed on the surface, with a density profile as shown in Fig. 1. For the case where a single reaction describes receptor-ligand interactions in the system (receptor and ligand binding to form a complex), the total number of complexes in the system at equilibrium can be calculated from a spatially dependent mass action law. Neglecting steric interactions between receptors, the receptor-ligand binding reaction at equilibrium is governed by:

$$\rho_c^{2D} = \rho_L^{2D} \rho_R^{2D} / K_D^{2D}, \quad (1)$$

where  $\rho_c^{2D}$ ,  $\rho_r^{2D}$ , and  $\rho_L^{2D}$  are the densities (number/area) of receptor-ligand complexes, unoccupied receptors, and unoccupied ligand, respectively, and  $K_D^{2D}$  is the 2D equilibrium dissociation constant, with units of number/area. Because receptors are free to diffuse throughout the interface, the free receptor concentration profile is spatially invariant at equilibrium; diffusion will continue to adjust the local unbound receptor concentration to maintain a flat density profile as ligand binding occurs. The line density of immobilized ligands,  $\rho_L^{2D}(x, y)$ , is a function of the planar coordinates  $x, y$  and is modeled as a 2D step function for the clustered ligand surfaces. The parameters describing this function are the amplitude  $\rho_{L,C}$  (local number of ligands within a cluster per unit area), cluster size (length per side of the cluster)  $D$ , and cluster separation  $d$ . For a total number of clusters  $n$  within the interface and a total area of interface  $X = n(D + d)^2$ , the (average) total ligand density is:

$$\langle \rho_L^{2D} \rangle = nD^2 \rho_{L,C}^{2D} / X. \quad (2)$$

For clustered ligand, the receptor-ligand complex line density,  $\rho_C^{2D}(x, y)$ , will also depend on  $x$  and  $y$ . As shown in Fig. 1,  $\rho_C^{2D}(x, y)$  is a 2D step function:

$$\rho_C^{2D}(x, y) = \begin{cases} \rho_{C,C}^{2D} = \rho_{L,C}^{2D}\rho_R^{2D}/K_D^{2D}, & \text{for } x, y \text{ within clusters} \\ 0 & \text{elsewhere} \end{cases} \quad (3)$$

for  $x, y$  within clusters elsewhere. The free receptor density,  $\rho_R^{2D}$ , is independent of  $x$  and  $y$  everywhere in the interface and is related to total initial receptor density,  $\rho_{R,TC}^{2D}$ , according to:

$$\rho_R^{2D} = \rho_{R,T}^{2D} - \langle \rho_C^{2D} \rangle = \rho_{R,T}^{2D} - (nD^2\rho_{C,C}^{2D})/X. \quad (4)$$

Substituting Eq. 4 into Eq. 3, we obtain for the local concentration  $\rho_{C,C}^{2D}$  of complexes within a cluster:

$$\rho_{C,C}^{2D} = \rho_{L,C}^{2D}\rho_{R,T}^{2D}/(K_D^{2D} + \langle \rho_L^{2D} \rangle). \quad (5)$$

The total number of complexes  $C$  in the interface becomes:

$$\begin{aligned} C &= X \sum \rho_C^{2D}(x, y) = nD\rho_{C,C}^{2D} \\ &= (X\langle \rho_L^{2D} \rangle \rho_{R,T}^{2D})/K_D^{2D} + \langle \rho_L^{2D} \rangle. \end{aligned} \quad (6)$$

This expression is exactly equivalent to the result expected for the case of a homogeneous distribution of ligand where  $\rho_L^{2D}(x) = \langle \rho_L^{2D} \rangle$  for all  $x$ . Thus, clustering ligand without changing the nature of receptor-ligand interactions (or introducing other molecules for receptors to interact with) does not increase the total number of complexes formed. Comparing the same total density of ligand clustered versus unclustered, the total number of complexes formed is the same because the local increase in  $\rho_C^{2D}$  induced by increased ligand concentration within clusters is exactly offset by the decrease in ligand density outside the clusters. Only local complex densities (within clusters) can be affected by clustering. The local complex density within ligand clusters ( $\rho_{C,C}^{2D}$ ) in terms of the mean complex density for the same total amount of ligand distributed randomly ( $\rho_{C,U}^{2D}$ ) is:

$$\rho_{C,C}^{2D} = (\rho_{L,C}^{2D}\rho_{R,T}^{2D})/\langle \rho_L^{2D} \rangle = (X\rho_{C,U}^{2D})/nD^2. \quad (7)$$

For example, nanoscale clustering of 5 ligands within a 400-nm<sup>2</sup> area, at a total ligand density of 500 ligands/ $\mu\text{m}^2$ , would give an increase in local complex density within clusters of 25 times the average total complex density on a surface with a homogeneous random ligand distribution. It should be emphasized, however, that steric interactions between receptors within a single cluster are not accounted for in this model and may influence this result.

## MONTE CARLO SIMULATIONS

### Model description

To probe the role of steric effects as well as binding affinity effects with varying ligand spatial distribution, we devel-

oped a Monte Carlo simulation of integrin-ligand complex formation at the cell-substrate interface. The model is schematically shown in Fig. 1. The contact area of the cell membrane against the substrate is modeled as a planar square lattice (500  $\times$  500 sites). Coarse-graining the model at the level of 100 nm<sup>2</sup> of surface area per lattice site (approximately the size of integrin receptors (Chothia and Jones 1997)), gives a total model area of 25  $\mu\text{m}^2$ ,  $\sim$ 2.5% of the total real area of contact ( $\sim$ 1000  $\mu\text{m}^2$  (Bell et al., 1984)) of a spread fibroblast on a substrate. The lattice size was chosen to minimize finite size effects in the simulation results; however, we found no variation in the measured parameters for a variety of total ligand/receptor densities and cluster sizes for lattices of 500  $\times$  500, 200  $\times$  200 (4  $\mu\text{m}^2$ ), or 100  $\times$  100 (1  $\mu\text{m}^2$ ) sites. Diffusion of receptors or ligand in the third dimension (i.e., orthogonal to the plane of the cell-substrate interface) has been neglected, as the separation between the cell membrane and the surface is small relative to the lateral dimensions of the lattice.

The lattice is occupied by three components: tethered (immobilized) ligands, mobile cell surface receptors, and immobilized receptor-ligand complexes. The number of receptors on the lattice is fixed at 2500 (100 integrins/ $\mu\text{m}^2$ ), corresponding to a typical integrin expression level of 100,000 receptors/cell (Bell et al., 1984; Ward and Hammer, 1993). A ligand or complex located on a given lattice site is immobilized to that 100-nm<sup>2</sup> area. Receptor diffusion in the cell membrane is modeled by allowing receptors (labeled R in the schematic) to move during the simulation to nearest-neighbor sites on the lattice. When a receptor diffuses onto a site occupied by a ligand, a complex is formed (C in the schematic). Volume exclusion of the receptors and complexes is maintained by disallowing moves that place one receptor in the same lattice site as another free receptor or complex. To minimize finite size effects, periodic boundary conditions are employed at the edges of the lattice.

The spatial distribution of ligands is determined at the outset of the simulation and remains static during equilibration of the system. The ligand spatial distribution for a given simulation is determined by the total fraction of lattice sites to be occupied by ligand and the cluster size  $D$ . Ligand clusters are fixed as  $D \times D$  square arrays, where  $D$  is the number of sites along one side (i.e.,  $D = 3 \rightarrow 3 \times 3$  arrays of ligand, occupying 900 nm<sup>2</sup>). At the outset of the simulation, clusters are placed randomly on the lattice in a manner preserving volume exclusion of the ligands (only one ligand is allowed to occupy any given site), until the prescribed fraction of lattice sites is filled. Unclustered ligand presentation is modeled by setting  $D = 1$ . Total ligand densities in simulations were varied two orders of magnitude from 30 ligands/ $\mu\text{m}^2$  to 4000 ligands/ $\mu\text{m}^2$ . After placing ligands, receptors are also initially placed randomly on the lattice, on unoccupied sites, until 2500 receptors (100 receptors/ $\mu\text{m}^2$ ) are allocated.

Dynamics of the system and evolution toward the equilibrium state are simulated by diffusion of receptors and receptor-ligand binding/unbinding. At each cycle of the simulation, a receptor and move direction (up, down, left, or right) are randomly chosen, and the attempted move is accepted or rejected according to excluded volume constraints and the Metropolis criterion. The Metropolis criterion ensures sampling of the equilibrium distribution of the system (Binder 1997; Metropolis et al., 1953) by setting the probability for accepting a move of a receptor based on energetic interactions between the components of the system. The energy of receptors is defined here to be 0 in the unbound state, whereas the energy of the receptor-ligand complex is  $E$  ( $E < 0$ ). Moves that leave the energy of the system unchanged or which lower the energy of the system are automatically accepted. Thus, moves of unbound receptors through the lattice or moves of an unbound receptor onto a free ligand (forming a complex) are accepted with unit probability. Diffusion of a receptor off a ligand site (breaking a receptor-ligand bond) is allowed with probability  $p = \exp(-\Delta E/kT) = \exp(E/kT)$ ; the energetically unfavorable process of breaking the ligand-receptor bond is allowed, but only with a likelihood determined by a Boltzmann weight for the bound state. Simulations using one binding energy to describe receptor-ligand interactions are hereafter referred to as the single-state model.

### Modeling complex-complex interactions

To examine the effect of possible binding energy changes due to clustering of ligated receptors, a two-state binding energy model was used. Two different energies for the bound receptor state were introduced,  $E_1$  and  $E_2$  ( $E_2 < E_1 < 0$ ), which represent the energy of discrete receptor-ligand pairs and clustered complexes, respectively. Clustering changes the binding energy via nearest-neighbor complex interactions: complexes that form adjacent to an existing receptor-ligand pair break with a probability  $p_2 = \exp(E_2/kT)$ , whereas discrete complexes break with probability  $p_1 = \exp(E_1/kT)$  ( $p_2 < p_1$ ). This simple model accounts for an effective increase in the affinity of receptor-ligand interactions within clusters. Further, because methods developed for measuring 2D kinetic parameters (on/off rates) (Chesla et al., 1998; Piper et al., 1998) have not yet to our knowledge been applied to integrin-adhesion ligand interactions, we estimate our kinetic parameters using 3D solution values for affinity constants.

We consider a relatively wide physiological range of ligand affinities based on published solution  $K_D$  values for ECM proteins and synthetic RGD-containing adhesion peptides. ECM proteins such as fibronectin represent the high-affinity extreme, with solution  $K_D$  values of  $10^{-7}$  to  $10^{-6}$  M. Synthetic cyclic and linear peptides represent the middle and low-affinity regimes, with  $K_D$  values of  $10^{-5}$  to  $10^{-3}$  M (Ruoslahti, 1996; Xiao and Truskey, 1996). Simulations

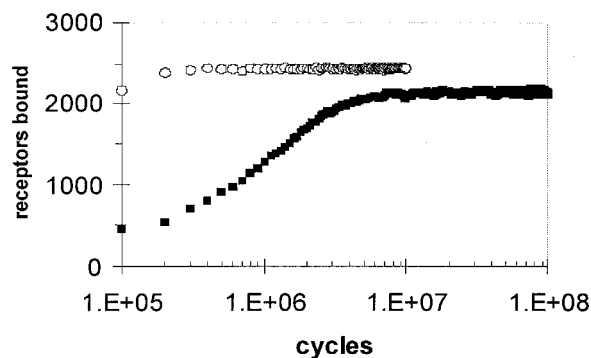


FIGURE 2 Evolution of equilibrium state for two example simulations: ○, instantaneous number of bound receptors for an example single-state simulation (cluster size = 1, ligand density  $100/\mu\text{m}^2$ , 2500 receptors, and  $E = -2.0kT$ ); ■, bound receptors for an example two-state simulation ( $D = 5$ , 1000 ligands/ $\mu\text{m}^2$ , 2500 receptors/ $\mu\text{m}^2$ ,  $E_1 = -2.0kT$  and  $E_2 = -6.0kT$ ).

were run using discrete receptor-ligand binding energies  $E_1$  corresponding with these solution  $K_D$  values. To model the low-affinity regime (corresponding to tethered RGD peptides),  $E_1$  was set to  $-1.0kT$  ( $K_D \approx 2 \times 10^{-4}$  M), whereas the high-affinity regime (corresponding to substrate-bound ECM proteins) was modeled by  $E_1 = -5.0kT$  ( $K_D \approx 3.7 \times 10^{-6}$  M). To investigate the effects of increased affinity on clustering, the clustered-state binding energy  $E_2$  is varied from  $1E_1$  to  $8E_1$ .

### Equilibration of systems

Equilibration is effected by repeating the cycle of receptor selection and attempted movement. The equilibrium state of the system evolves after many Monte Carlo (MC) steps, defined as the average number of cycles required to randomly select and attempt moving each receptor once. For the receptor density studied ( $100$  receptors/ $\mu\text{m}^2$ ), the average number of cycles per MC step is  $\sim 20,000$ . Given known diffusivities of membrane receptors ( $10^{-9}$  to  $10^{-10}$   $\text{cm}^2/\text{s}$ ) (Lauffenburger and Linderman, 1993), one Monte Carlo step is correlated with  $\sim 100$ – $1000$   $\mu\text{s}$  of real time. From the stochastic initial receptor distributions, equilibrium was achieved within  $\sim 250$  MC steps for clustered ligand systems, and much faster for unclustered distributions ( $D = 1$ ). This corresponds to real times on the order of a few seconds. Two representative examples illustrating system equilibration are shown in Fig. 2, where the instantaneous percent of bound receptors for  $D = 1$  in the single-state model and  $D = 5$  in the two-state model are shown.

Equilibrium values for system properties were determined by averaging steady-state values over  $10^8$  cycles (beginning after  $10^7$  cycles for equilibration) for three separate random cluster distributions. The primary attributes of interest for each simulation are the number of receptors (or fraction of receptors) bound at equilibrium and the number of receptors per cluster.

## Relationship between model parameters and solution affinities

The equilibrium receptor-ligand dissociation constant  $K_D$  is related to the bond break probability  $p$ . At equilibrium, the number of bonds formed per unit time must equal the number of bonds broken. For the lattice model, this is expressed as:

$$(p_{\text{on}}/\tau)(\rho_L A/N^2)((\rho_R - \rho_C)A/N^2) = (p_{\text{off}}/\tau)(\rho_C A/N^2), \quad (8)$$

where  $p_{\text{on}}$  is the instantaneous probability for bond formation per site occupied by both receptor and ligand,  $p_{\text{off}}$  is the probability of breaking a receptor-ligand complex,  $\tau$  is the amount of real time per MC step,  $\rho_L$  is the total ligand surface density,  $\rho_R$  is the total receptor surface density,  $\rho_C$  is the average complex surface density,  $A$  is the area modeled, and  $N^2$  is the total number of lattice sites in the model ( $N$  sites per side in the lattice). The quantities  $(\rho_L A/N^2)$ ,  $((\rho_R - \rho_C)A/N^2)$ , and  $(\rho_C A/N^2)$  are probabilities a given site on the lattice is occupied by a ligand, unbound receptor, or complex, respectively. The bond formation/break probabilities  $p_{\text{on}}$  and  $p_{\text{off}}$  are:

$$p_{\text{on}} = 1 \quad (9)$$

$$p_{\text{off}} = p = e^{-\Delta E/kT} \quad (10)$$

Equation 8 is the lattice equivalent of the real-space mass action equation:

$$k_{\text{on}}\rho_L(\rho_R - \rho_C) = k_{\text{off}}\rho_C \quad (11)$$

Thus, the bond break probability  $p$  is related to the two-dimensional affinity constant  $K_D^{2D}$ :

$$K_D^{2D} = k_{\text{off}}/k_{\text{on}} = \rho_L(\rho_R - \rho_C)/\rho_C = p/a = [\text{area}^{-1}], \quad (12)$$

where  $a$  is the area per lattice site ( $= A/N^2 = 1 \times 10^{-12}$  cm<sup>2</sup>/site).  $K_D^{2D}$  can in turn be related to the standard solution 3D  $K_D$  by considering the volume of the surface-localized receptor-ligand interactions. We assume the cell-substrate interface is planar in this model with a separation  $d \approx 300 \times 10^{-8}$  cm, consistent with the separation required for receptor-ligand interactions (Lauffenburger and Linderman, 1993). The 3D  $K_D$  is (in its standard units, assuming  $K_D^{2D}$  is in units of cm<sup>-2</sup>):

$$K_D = (1000K_D^{2D})/(dN_a) = (1000p)/(daN_a) = [\text{mol/L}], \quad (13)$$

where  $N_a$  is Avogadro's number. Using our model parameters for  $d$  and  $a$ , the 3D  $K_D = 5.53 \times 10^{-4}p$ .

## SIMULATION RESULTS

### Single-state binding models

According to the single-state binding analytical model presented above, no increase in the total number of

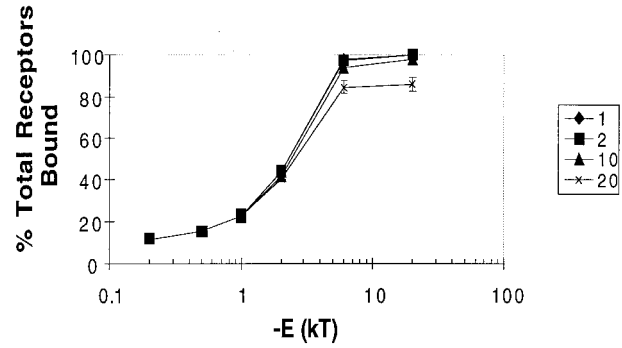


FIGURE 3 Monte Carlo results for receptor binding on clustered ligand surfaces using single-state model. Simulations were done with  $10^3$  ligands/ $\mu\text{m}^2$  and 100 receptors/ $\mu\text{m}^2$  at the cell-substrate interface. Equilibrium fraction of receptors bound was determined for four cluster sizes:  $D = 1, 2, 10,$  and  $20$ .

complexes is expected when ligand is clustered compared with a random ligand distribution. However, the analytical model neglects effects of receptor-receptor or receptor-complex steric interactions (receptor crowding or blocking within clusters). In MC simulations, such excluded volume interactions are readily accounted for. Simulation results for the fraction of available receptors bound at equilibrium for  $D = 1, 2, 10,$  and  $20$  are shown in Fig. 3 for the case of excess ligand ( $\rho_L = 10\rho_R$ ). In agreement with the analytical model, the simulations predict no increase in receptor binding by ligand clustering for a range of binding energies spanning from very weak binding ( $E = -0.2kT$ ,  $p \approx 0.80$ ,  $K_D = 4.42 \times 10^{-4}$  M) to moderate binding ( $E = -6.0kT$ ,  $p \approx 0.0025$ ,  $K_D = 1.38 \times 10^{-6}$  M). At very high binding energies (e.g.,  $E = -20kT$ ,  $p \approx 2.0 \times 10^{-9}$ ,  $K_D = 1.14 \times 10^{-12}$  M), however, the fraction of receptors bound actually decreases for larger clusters. This is caused by rings of tightly bound complexes at the cluster perimeter that sterically block entry of additional receptors into the cluster interior. Fig. 4 illustrates this effect for a system with  $D = 20$  at high binding energy ( $E = -20kT$ ) compared with a simulation of the same cluster size at a low binding energy ( $E = -2.0kT$ ). Although the ringed cluster structures are metastable (nonequilibrium), some receptor-ligand pairs are known to bind with even higher affinity (e.g., avidin-biotin,  $K_D \approx 10^{-15}$  M (Chilkoti and Stayton, 1995; Weber et al., 1989)). For high-affinity binding these long-lived metastable states may persist through experimentally relevant timescales. Ring structures of larger size than those described here have been observed experimentally for adhesion of hepatocytes to high-density carbohydrate ligand surfaces via the asialoglycoprotein receptor, which has an affinity of  $1 \times 10^{-9}$  to  $10 \times 10^{-9}$  M (i.e.,  $\sim 1000$ -fold higher affinity than that we consider here).

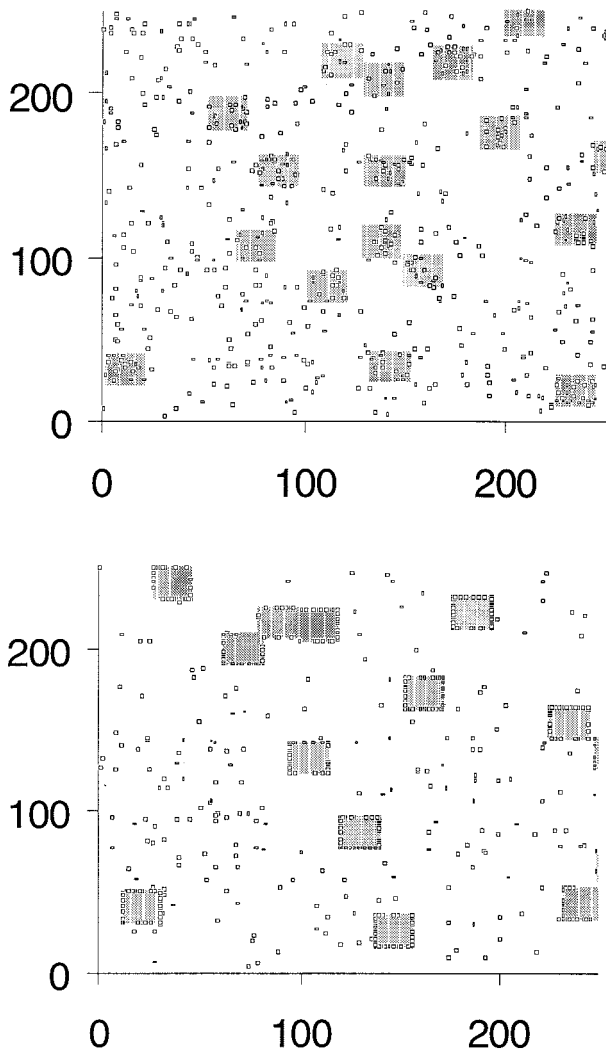


FIGURE 4 Steric blocking of ligand for high receptor-ligand affinities. Shown are snapshots of ligand and receptor lattice distribution from equilibrated systems for two systems having  $100 \text{ receptors}/\mu\text{m}^2$  and  $1000 \text{ ligands}/\mu\text{m}^2$ . (A) A low-binding-energy simulation:  $E = -2.0kT$ . Receptors access ligand throughout clusters. (B) Ligand in the interior of clusters is blocked in a high affinity system:  $E = -20kT$ .

### Two-state receptor binding model in conjunction with ligand clustering

Next, the role of clustering was investigated assuming that nearest-neighbor complexes bind with a greater energy than isolated receptor-ligand pairs. Simulations were carried out for a range of total ligand densities with discrete- and clustered-state binding energies  $E_1$  and  $E_2$ , respectively. From these simulations, two regimes of receptor binding were identified: for high ligand densities ( $\rho_L \approx 10\rho_R$  or greater), receptor binding increases with increasing cluster size up to  $D = 5$ , beyond which binding is saturated. At lower total ligand densities, a different qualitative trend is followed. For  $\rho_L < 10\rho_R$ , a maximum in receptor binding is

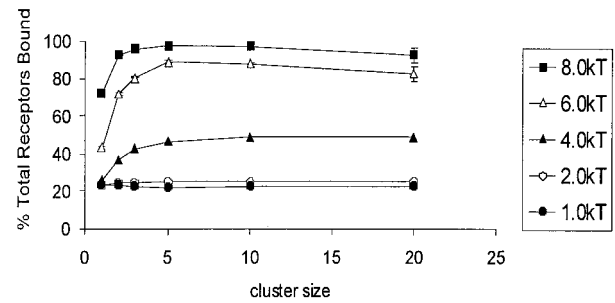


FIGURE 5 Receptor binding in two-state model for low discrete-state binding affinity. Average percent of total available receptors bound at equilibrium from Monte Carlo simulations is plotted versus cluster size for a series of clustered-state binding energies at  $\rho_L = 1000/\mu\text{m}^2$ . Binding energies:  $-E_1$  was fixed at  $1.0kT$  whereas  $-E_2$  was varied as shown in the legend.

observed at intermediate cluster sizes  $D = 3-5$ , with a decrease in binding at larger cluster sizes, due to steric blocking of interior ligand sites of large clusters. In both of these regimes, binding energies and total ligand density control how many complexes are formed at maximum binding and at what cluster size maximal binding occurs.

The effect of ligand clustering on receptor binding for a low discrete-state binding energy (modeling low-affinity peptide ligands) is seen in Fig. 5, which shows the percent of available receptors bound at equilibrium for  $E_1 = -1.0kT$  as  $E_2$  is varied from  $-1.0kT$  to  $-8.0kT$  for the case  $\rho_L = 10\rho_R$ . A clustered-state binding energy of  $E_2 = 4E_1$  gives rise to approximately twice the number of bound receptors for  $D \geq 5$ . Significant increases in receptor binding versus the unclustered ( $D = 1$ ) case occur even for small clusters of only four ligands per group. When 25 or more ligands are clustered ( $D \geq 5$ ), receptor binding plateaus. The magnitude of  $E_2$  controls the fraction of bound receptors. The effects of the relative magnitudes of  $E_2$  and  $E_1$  are better seen in Fig. 6, where percent receptors bound is replotted for different cluster sizes versus  $E_2/E_1$ . For a small perturbation in the binding energy ( $E_2/E_1 = 2$ ), there is little or no effect of clustering ligand. However, over a range of  $E_2/E_1 = \sim 4-8$ , ligand clustering results in formation of a greater number of complexes, up to approximately twice the number of complexes obtained on unclustered ( $D = 1$ ) surfaces.

In addition to increasing the fraction of bound receptors, ligand clustering in the two-state model also drives the aggregation of receptors. Fig. 7 A shows the average number of receptors per cluster calculated from simulation results for the single-state model (with  $E = -1.0kT$ ) compared with the two-state model ( $E_1 = -1.0kT$ ,  $E_2 = -6.0kT$ ) for  $\rho_L = 1000/\mu\text{m}^2$ . Two-state binding drives clustering of receptors much more efficiently than a one-state process (by a factor of  $\sim 5$  at all cluster sizes). Even at this high ligand density, the single-state binding model yields no more than one receptor per cluster for  $D < 5$ . In

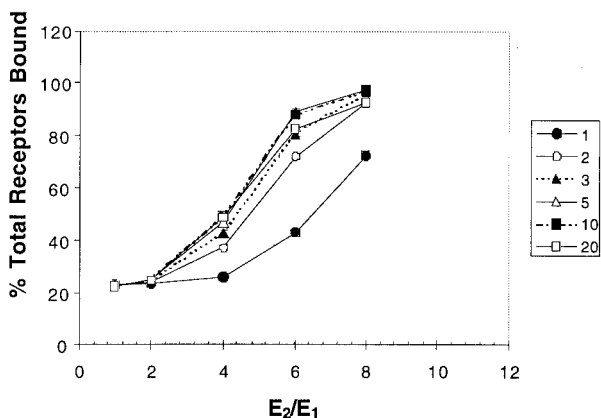


FIGURE 6 Relative strength of clustered versus unclustered binding energy strongly influences receptor binding for the two-state binding model. Shown are simulation results for total ligand density  $1000/\mu\text{m}^2$ ,  $E_1 = -1.0kT$ , and a range of cluster sizes as denoted by the legend.

contrast, multiple receptors are bound for  $D = 3-5$  using the two-state model. Fig. 7 B shows the average number of receptors/cluster for a range of total ligand densities and cluster sizes in the two-state model for  $E_1 = -1.0kT$  and  $E_2 = -6.0kT$ . Clustering ligand in this case significantly increases the number of receptors/cluster over the entire range of ligand densities.

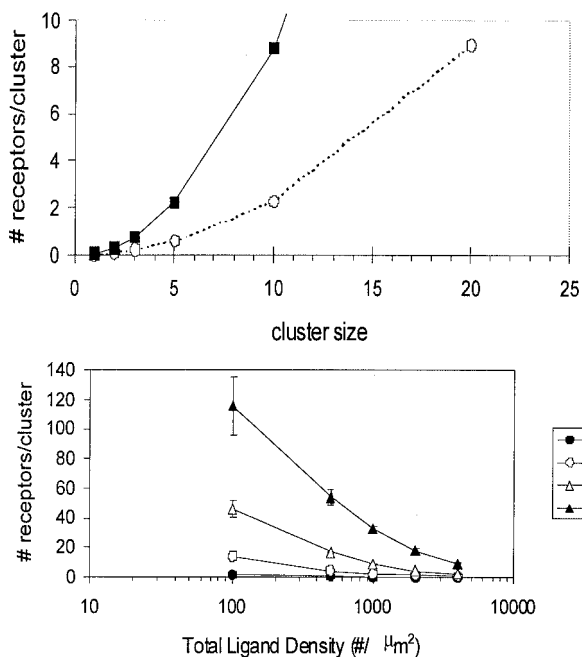


FIGURE 7 Receptor clustering induced by ligand clustering. (A) Average number of receptors per cluster is compared for the single-state binding model ( $\circ$ ,  $E = -1.0kT$ ) or the two-state binding model ( $\blacksquare$ ,  $E_1 = -1.0kT$ ,  $E_2 = -6.0kT$ ) at a total ligand density of  $1000/\mu\text{m}^2$ . (B) The average number of receptors per cluster from Monte Carlo simulations of two-state model with  $E_1 = -1.0kT$  and  $E_2 = -6.0kT$  is plotted for cluster sizes as denoted in the legend.

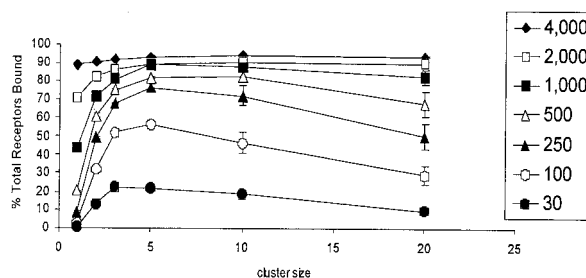


FIGURE 8 Effect of ligand concentration on receptor binding in two-state model. Average percent of total available receptors bound at equilibrium from simulations is plotted versus cluster size for fixed binding energies  $E_1 = -1.0kT$ ,  $E_2 = -6.0kT$ . Data is shown for a range of total ligand densities from  $30 \text{ ligands}/\mu\text{m}^2$  to  $4,000 \text{ ligands}/\mu\text{m}^2$  as denoted in the legend.

### Role of total ligand concentration

Total ligand concentration plays an important role in the pattern of receptor binding in the two-state binding model. Simulations were run with binding energies  $E_1 = -1.0kT$  and  $E_2 = -6.0kT$ . Fig. 8 shows the fraction of receptors bound versus cluster size for total ligand densities ranging from  $30 \text{ ligands}/\mu\text{m}^2$  up to  $4000 \text{ ligands}/\mu\text{m}^2$ . At low  $\rho_L$  the trend of receptor binding with increasing cluster size is biphasic, due to the competition between receptors for a finite number of available cluster perimeter sites. In contrast, at high  $\rho_L$ , all surfaces approach maximal binding of available receptors and clustering does not significantly increase the level of receptor binding relative to the unclustered case. This is seen in Fig. 9 where data are replotted to show total receptor binding at constant cluster size as total ligand density is varied. For total ligand densities  $\geq 4000/\mu\text{m}^2$ , clustering effects appear insignificant.

Even random ligand distributions, such as are likely obtained by most methods of peptide or protein surface immobilization, show a nonlinear dependence of bond number on ligand density if clustering increases the effective receptor-ligand affinity. Plotted in Fig. 9 is the binding profile for

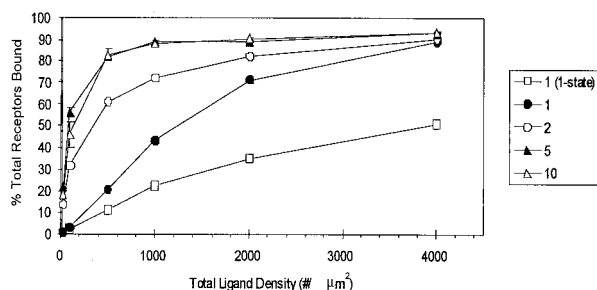


FIGURE 9 Receptor binding profiles for constant cluster size. Simulation results using  $-E_1 = 1.0kT$  and  $-E_2 = 6.0kT$ . Shown is the percent receptors bound from simulations for  $D = 1-10$  as denoted by legend. Also plotted for comparison is the binding curve for  $D = 1$  in the one-state binding model with  $-E = 1.0kT$ .

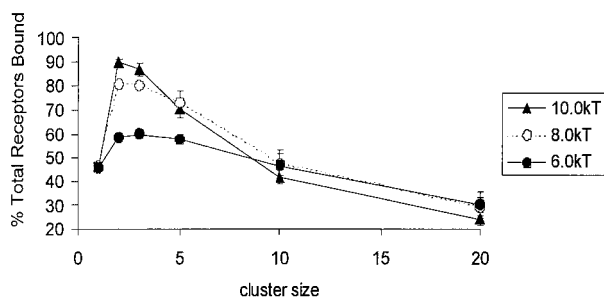


FIGURE 10 Receptor binding in two-state model for high discrete-state binding affinity. Average percent of total available receptors bound at equilibrium from Monte Carlo simulations is plotted versus cluster size for a series of clustered-state binding energies at  $\rho_L = 1000/\mu\text{m}^2$ . For binding energies,  $-E_1$  was fixed at  $5.0kT$  whereas  $-E_2$  was varied as shown in the legend.

unclustered ( $D = 1$ , open squares) ligand in the single-state model with  $E = -1.0kT$ . The unclustered single-state simulation shows significantly fewer receptor-ligand bonds than the same unclustered ligand distribution in the two-state model ( $E_1 = -1.0kT$ ,  $E_2 = -6.0kT$ ; filled circles). This is because as ligand density increases, a stochastic distribution of the ligand gives rise to an increasing number of nearest-neighbor ligands and thus increased receptor binding due to nearest-neighbor complex contacts.

### High-affinity versus low-affinity discrete-state binding

To model clustering of ECM protein ligands such as fibronectin, which have a significantly higher binding affinity for integrins, we also performed simulations where the initial unclustered-state binding energy was significantly larger,  $E_1 = -5.0kT$ . At the ligand density plotted in Fig. 3 ( $1000 \text{ ligands}/\mu\text{m}^2$ , or  $\rho_L = 10\rho_R$ ), such a high-affinity ligand will bind nearly all available receptors even in the unclustered state. However, clustering effects are observed at lower total ligand densities. Fig. 10 shows the percent receptors bound at a total ligand density of  $100 \text{ ligands}/\mu\text{m}^2$  ( $\rho_L = \rho_R$ ) as a function of cluster size for  $E_1 = -5.0kT$  and  $E_2 = -6-10kT$ . Receptor binding exhibits a maximum as cluster size is varied, similar to the pattern observed for lower values of  $E_1$  in Fig. 8, whereas increasing  $E_2$  increases the maximum percent receptors bound. Small degrees of clustering are found to dramatically increase the level of receptor binding due to the increased affinity on clustering. For large cluster sizes, however, the number of receptors exceeds the number of perimeter cluster sites. Thus, complex formation around the perimeter blocks access to interior sites, causing a decrease in the fraction of bound receptors for  $D > 5$ . These metastable ringed states, as illustrated in Fig. 4 B, persist for extremely long times (greater than the  $10^8$  cycles in our simulations) and may indicate that at low

ligand densities, when  $|E_2| > 4-6kT$ , an optimal cluster size exists regardless of the value of  $E_1$ .

## DISCUSSION

### Models for integrin clustering

The formation of focal or localized adhesions between cells and matrix observed in culture and in vivo requires aggregation of integrin adhesion receptors. Understanding the role specific molecular parameters play in the process of focal adhesion formation allows design of strategies to influence this process for therapeutic or diagnostic applications. One biophysical process that might give rise to receptor clustering is a positive cooperative effect of receptor binding to the substrate. This effect was first analyzed by Segel and co-workers (1983), who were motivated by observations of the periodicity of cell-substrate adhesion structures forming at the periphery of spreading cells during the initial phase of spreading. Using a perturbation analysis of cooperative receptor binding in a large excess of uniformly distributed ligand, they predicted that small clusters could grow for certain combinations of physical parameters (free receptor diffusion coefficient, receptor/ligand on/off rates, and receptor-ligand complex effective diffusion coefficient) and relax toward uniformity for others. Although their analysis was not amenable to predicting equilibrium structures or showing effects for specific parameter values, as we do here, the model of Segel and co-workers provides an important conceptual basis for cooperative effects on focal contact formation.

A more detailed model that accounts for quantitative effects of intracellular molecular associations between integrin cytoplasmic tails and talin, self-aggregation of talin, and extracellular receptor-ligand affinities on focal adhesion formation was developed by Ward and Hammer (1994). They examined the steady-state number of molecular aggregates in the context of a uniformly distributed but systematically varied density of extracellular integrin ligand. They predicted that within a physiological range of parameter values, the affinity of talin-talin interactions exerts a dominating effect on the aggregation process when extracellular ligand concentrations are sufficiently high (Ward and Hammer, 1994). Signaling processes initiated by integrin ligation may induce changes in talin affinities via phosphorylation events, providing a means to control integrin aggregation and focal adhesion formation.

Our focus here is how spatial effects in the extracellular environment might influence the aggregation process. Given the recent experimental evidence that ligand clustering alters integrin-mediated cell behaviors, including adhesion strength, cytoskeletal organization, and migration speed (Maheshwari et al., 2000), we sought to simulate focal contact formation using a biophysical model that captures some key aspects of the experimental system,

ligand clustering under conditions of either limiting or saturating ligand (relative to receptor density), and cooperative binding, with receptor-ligand affinity constants in a physiological range for integrin-matrix binding. Monte Carlo methods provide a useful tool for capturing the spatial effects. We represented the cooperativity effects as an increase in receptor-ligand affinity in the case of adjacent bound receptors compared with lone bound receptors, using a physiological range of integrin affinities. This conceptually captures the idea of neighbor effects that might be mediated through intracellular molecules such as talin in a form amenable to Monte Carlo simulation.

Simulations indicate that if receptor-ligand binding occurs with no change in binding affinity of neighboring ligands, the total number of receptors bound remains constant when comparing ligand presented in clusters versus homogeneously distributed on the substrate. However, the local surface concentration of complexes at sites of ligand clustering is higher, which may itself facilitate focal contact formation due to the relative increase in local integrin concentration at such points of contact.

Several factors can influence the apparent affinity of integrins for extracellular ligands, including exogenous activation by antibodies or  $\text{MnCl}_2$  (Frelinger et al., 1991; Ginsberg et al., 1992). Global increases in integrin affinity resulting from such activation, however, would not give rise to the strong effects of clustering on receptor occupation that we observe in our two-state model, which presumes changes in effective integrin affinity occur locally. Such local changes would be experimentally difficult to observe directly. However, the presence of secondary interactions between ligated integrins and other molecular components can be expected to increase the effective affinity of the receptor for ligand immobilized on a substrate. Integrin activation states could be controlled by integrin-cytoskeleton interactions, receptor-receptor interactions, or interactions between integrins and other locally active cytosolic partners such as kinases or phosphatases (Ginsberg et al., 1992; Huttenlocher et al., 1996). Indirect evidence that receptor activation may arise from interaction of ligated receptors can be found in the observations by Danen et al. (1995) that unactivated  $\alpha_5\beta_1$  requires the PHSRN synergy site for binding to GRGDSP fibronectin peptide, but exogenously activated  $\alpha_5\beta_1$  was able to bind GRGDSP in the absence of the synergy site. One interpretation of these results is that the synergy site induces clustering of integrins; this interpretation could be tested by creating a peptide with two GRGDSP sequences presented at equal spacing as the constructs containing PHSRN and GRGDSP used by Danen et al. (1995). Likewise, Chi-Rosso et al. (1997) observed that activation of  $\beta_1$ -integrins enabled binding to fibronectin type III repeats that lacked the RGD sequence, again suggesting that multivalent interactions are perhaps required when integrins are not pre-activated.

Physical immobilization of receptors by recruited scaffolding proteins or elements of the cytoskeleton may also increase effective receptor-ligand affinities. In addition to talin, the membrane protein calveolin-1 also serves as a macromolecular cross-linker, aiding in the process of integrin clustering on the cell membrane side of the interface (Wary et al., 1998; Wei et al., 1999). These multiple interactions between integrins and cytosolic components or other receptors are likely to act cooperatively to control receptor binding. As an example, Shaw et al. (1990) demonstrated that spreading of macrophages on laminin is triggered only under conditions where  $\alpha_6\beta_1$  integrin is clustered in focal contacts, attached to actin fibers of the cytoskeleton, and phosphorylated due to an exogenous signal.

Using a two-state binding energy model, we have modeled in the simplest possible fashion such higher-order effects that occur in cell adhesion beyond simple receptor ligation. Two main conclusions are drawn from simulations of two-state binding. First, modest changes in the binding energy on receptor clustering significantly increase receptor binding on clustered ligand surfaces relative to random unimolecular ligand distributions. Increases in the binding energy corresponding to solution  $K_D$  changes of about a factor of 10 for unclustered versus clustered binding give two to three times more bound receptors over a broad range of ligand densities. This relative increase in receptor binding occurs for even very low-affinity discrete receptor-ligand pairs and occurs for even small cluster sizes. These model predictions are consistent with the experimental observations of cells migrating on random or clustered low-affinity adhesion peptide (Maheshwari et al., 2000), where random peptide was ineffective whereas clustering resulted in migration speeds comparable to those on fibronectin.

As shown in Fig. 9, receptor binding is most sensitive to clustering at low total ligand densities, varying by an order of magnitude between unclustered and clustered ligand distributions. Second, as the ligand density becomes comparable to the receptor density in the interface, the model predicts the existence of an optimum cluster size (10–25 ligands/cluster), when  $E_2 \geq 6.0kT$ . The predicted decrease in receptor binding hinges on steric interactions between receptors and would not occur if receptors were able to shoulder their way through the crowded cluster perimeter or if the cytoskeleton actively rearranged receptors.

Fig. 6 indicates a weak dependence of clustering effects on cluster size. However, the present model considers only single nearest-neighbor complex-complex interactions, which may underestimate the possible changes in binding occurring with clustering. In real cells, multi-complex interactions may modify binding in a more complex manner, providing a large number of possible effective binding energies depending on the number of receptors in a cluster or upon second- or third-nearest-neighbor interactions. Ligand grouping might thus even more dramatically alter receptor binding for large clusters.

## Relation to experimental data

Theoretical treatments have predicted that cell adhesion strength is proportional to the number of bonds between the cell and its substrate (Dembo et al., 1988; Ward and Hammer, 1993) and whether bonds are isolated or aggregated in focal adhesions (Ward and Hammer 1993).

Experimental validation of whether apparent integrin-ligand binding interactions are single-state or two-state in the case of real clustered integrin-ligand interactions requires measurement of cell adhesion strengths on well-characterized surfaces presenting equal concentration of clustered versus unclustered ligands. If secondary interactions that modify the receptor-ligand affinity are important, then clustered ligand surfaces should show significant increases in adhesion strength compared with homogeneous or random ligand distributions at the same total amount of ligand. This increase in adhesion at a set average ligand density for the two-state model arises from two factors: 1) an increased fraction of receptors is bound in the case of clustered ligand, and 2) there is an increase in the affinity of each bond and, concomitantly, in the adhesion strength of each bond. Thus, even under conditions where all integrins are ligated, the two-state model predicts that the clustered ligand will induce greater adhesion strength compared with the randomly presented ligand due to the greater affinity of bonds. Recent experiments by Maheshwari et al. (2000) examining the adhesion strength of fibroblasts on nanoscale-clustered RGD peptides may be the first experimental evidence of such clustering effects. Using a star polymer of polyethylene oxide to cluster RGD ligands against an otherwise inert background, they presented an RGD adhesion ligand in clusters of 1 (i.e., random), 5, or 9 peptides per  $\sim 50$ -nm cluster and found dramatic increases in adhesion strength upon increasing ligand cluster size (Maheshwari et al., 2000). At equivalent total ligand densities, nine RGD/cluster surfaces gave increases in adhesion strength by a factor of two to three over unclustered ligand across two orders of magnitude in ligand density. Assuming that bond number is the primary determinant of adhesion strength, our model suggests that such dramatic effects require an increase in the effective receptor-ligand affinity upon clustering.

Maheshwari et al. (2000) also observed similar trends in stress fiber formation within cells adhering to clustered RGD surfaces: two to three times more cells on nine RGD/cluster surfaces showed well-developed stress fibers than on unclustered RGD surfaces at equal total RGD densities. This is intriguing, as the present simulations predict much stronger clustering of receptors in the two-state model relative to single-state binding. Assuming that multiple receptors per cluster is a requirement for focal contact formation, the two-state binding model is more consistent with the results seen by Maheshwari et al. (2000) than is the single-state model.

Our prediction that small ligand clusters will dramatically influence receptor binding and spatial distribution could also have important implications for the interpretation of results obtained on other model systems presenting tethered adhesion peptides that are assumed to be homogeneously distributed. For example, Xiao and Truskey (1996) measured cell adhesion strengths on silane-immobilized RGD peptides and found results consistent with a significant increase in receptor-ligand affinity for the ligands immobilized on the surface versus their solution  $K_D$ . Massia and Hubbell (1991) also reported that surprisingly low densities of RGD could support fibroblast spreading and focal contact formation on tethered-RGD surfaces, relative to results from other ligand immobilization schemes. The present simulations indicate that these observed increases in binding energy may be influenced in part by inadvertent ligand clustering, e.g., by silane oligomerization during surface preparation or other factors that lead to even small degrees of surface inhomogeneities. Small inhomogeneities in surface structure, even those arising from random juxtapositioning of ligands, may have strong effects on resulting adhesion strength.

Ligand clustering by ECM structures *in vivo* might be achieved in several ways. ECM proteins organized into fibrils, such as collagen and fibronectin, may present nanoscale ligand clusters to cells simply through the close spatial proximity of the assembled molecules. Cells actively assemble fibrils of ECM components such as fibronectin and collagen (Yamada et al., 1992), and strong integrin aggregation is observed during migration of highly adhesive cell types *in vivo* (Friedl and Bröcker, 2000b). Because cells bind to these proteins by multiple receptors during matrix assembly, ligand clusters could be created directly by cells; these clustered binding sites could then serve to drive clustering of integrins and focal contact formation. Alternatively, as shown in these simulations, adhesion proteins randomly adsorbed to an underlying basal lamina may present ligand clusters that trigger focal adhesion development at discrete sites.

Finally, for the development of novel biomaterials, these simulations indicate that if the binding energy of complexes is altered by clustering, increasing the number of ligands per cluster up to  $\sim 25$  ligands in  $2500 \text{ nm}^2$  increases receptor binding. Thus, ligand clustered in domains of sizes up to  $\sim 100 \text{ nm}$  may be effective in increasing the number of receptor-ligand bonds formed at the cell-substrate interface. A variety of approaches are feasible for preparing clustered ligand surfaces on such length scales. Immobilized multifunctional polymers have already been used to cluster ligands in  $10$ – $50$ -nm domains (Maheshwari et al., 2000). Block copolymers may express periodic surface domains with sizes on the order of a few tens of nanometers, which might serve as clustering templates (Fasolka et al., 1997). For larger-scale clustering domains, functionalized latex microspheres may be used to create  $100$ – $1000$ - $\mu\text{m}$  domains

of ligand at surfaces (Banerjee et al., 2000). Such nanoscale ligand clustering could be employed to control cell adhesion strength, manipulate cell migration rates, and control cell growth.

This work was supported in part by grants from the Whitaker Foundation grants RG-97-0196, NSF-DMR 98-17735, and NSF-BES9632714 and National Institutes of Health grant 1R0GM59870-01.

## REFERENCES

- Adams, J. C. 2001. Cell-matrix contact structures. *Cell. Mol. Life Sci.* 58:371-392.
- Aplin, A. E., A. Howe, S. K. Alahari, and R. L. Juliano. 1998. Signal transduction and signal modulation by cell adhesion receptors: the role of integrins, cadherins, immunoglobulin-cell adhesion molecules, and cadherins. *Pharmacol. Rev.* 50:197-263.
- Aukhil, I., P. Joshi, Y. Yan, and H. P. Erickson. 1993. Cell- and heparin-binding domains of the hexabrachion arm identified by teascin expression proteins. *J. Biol. Chem.* 268:2542-2553.
- Banerjee, P., D. J. Irvine, A. M. Mayes, and L. G. Griffith. 2000. Polymer latexes for controlling cell adhesion and receptor-mediated interactions. *J. Biomed. Mater. Res.* 50:331-339.
- Bell, G. I., M. Dembo, and P. Bongrand. 1984. Cell adhesion: competition between nonspecific repulsion and specific binding. *Biophys. J.* 45:1051-1064.
- Binder, K. 1997. Monte Carlo Simulations in Statistical Physics: An Introduction. Springer, New York.
- Burridge, K., and M. Chrzanowska-Wodnicka. 1996. Focal adhesions, contractility, and signaling. *Annu. Rev. Cell Dev. Biol.* 12:463-519.
- Chesla, S. E., P. Selvaraj, and C. Zhu. 1998. Measuring two-dimensional receptor-ligand binding kinetics by micropipette. *Biophys. J.* 75:1553-1572.
- Chi-Rosso, G., P. J. Gotwals, J. Yang, L. Ling, K. Jiang, B. Chao, D. P. Baker, L. C. Burkly, S. E. Fawell, and V. E. Kotliansky. 1997. Fibronectin type III repeats mediate RGD-independent adhesion and signaling through activated  $\beta_1$  integrins. *J. Biol. Chem.* 272:31447-31452.
- Chilkoti, A., and P. S. Stayton. 1995. Molecular origins of the slow streptavidin-biotin dissociation kinetics. *J. Am. Chem. Soc.* 117:10622-10628.
- Chothia, C., and E. Y. Jones. 1997. The molecular structure of cell adhesion molecules. *Annu. Rev. Biochem.* 66:823-862.
- Clark, E. A., and J. S. Brugge. 1995. Integrins and signal transduction pathways: the road taken. *Science.* 1995:233-239.
- Danen, E. H. J., S. Aota, A. A. van Kraats, K. M. Yamada, D. J. Ruitter, and G. N. P. van Muijen. 1995. Requirement for the synergy site for cell adhesion to fibronectin depends on the activation state of integrin  $\alpha_5\beta_1$ . *J. Biol. Chem.* 270:21612-21618.
- Danilov, Y. N., and R. L. Juliano. 1989. (Arg-Gly-Asp)N-albumin conjugates as model substratum for integrin-mediated cell-adhesion. *Exp. Cell. Res.* 182:186-196.
- de Panfilis, G., A. Ghindi, S. Graifemberghi, S. Barlati, N. Zoppi, and M. Colombi. 2000. Dexamethasone-induced healing of chronic leg ulcers in a patient with defective organization of the extracellular matrix of fibronectin. *Br. J. Dermatol.* 142:166-170.
- Dembo, M., D. C. Torney, K. Saxman, and D. Hammer. 1988. The reaction-limited kinetics of membrane-to-surface detachment. *Proc. R. Soc. Lond. B.* 234:55-83.
- Duband J-L, G. H. Nuckolls, A. Ishihara, T. Hasegawa, K. M. Yamada, J. P. Thiery, and K. Jacobson. 1988. Fibronectin receptor exhibits high lateral mobility in embryonic locomoting cells but is immobile in focal contacts and fibrillar streaks in stationary cells. *J. Cell Biol.* 107:1385-1396.
- Fasolka, M. K., D. J. Harris, A. M. Mayes, M. Yoon, and S. J. G. Mochrie. 1997. Observed substrate topography-mediated lateral patterning of diblock copolymer films. *Phys. Rev. Lett.* 79:3018-3021.
- Frelinger, A. L., X. P. Du, E. F. Plow, and M. H. Ginsberg. 1991. Monoclonal antibodies to ligand-occupied conformers of integrin  $\alpha_{IIb}\beta_3$  (glycoprotein IIb-IIIa) alter receptor affinity, specificity, and function. *J. Biol. Chem.* 266:17106-17111.
- Friedl, P., and E-B. Bröcker. 2000a. The biology of cell locomotion with three-dimensional extracellular matrix. *Cell. Mol. Life Sci.* 57:41-64.
- Friedl, P., and E. B. Bröcker. 2000b. The biology of cell locomotion within three-dimensional extracellular matrix. *Cell Mol. Life Sci.* 57:41-64.
- Ginsberg, M., X. Du, and E. F. Plow. 1992. Inside-out integrin signalling. *Curr. Opin. Cell Biol.* 4:766-771.
- Hato, T., N. Pampori, and S. J. Shattil. 1998. Complementary roles for receptor clustering and conformational change in the adhesive and signaling functions of integrin  $\alpha_{IIb}\beta_3$ . *J. Cell Biol.* 141:1685-1695.
- Huttenlocher, A., M. H. Ginsberg, and A. F. Horwitz. 1996. Modulation of cell migration by integrin-mediated cytoskeletal linkages and ligand-binding affinity. *J. Cell Biol.* 134:1551-1562.
- Hynes, R. O. 1999. Cell adhesion: old and new questions. *Trends Cell. Biol.* 24:M33-M37.
- Hynes, R. O., and K. M. Yamada. 1982. Fibronectins: multifunctional modular glycoproteins. *J. Cell Biol.* 95:369-377.
- Irvine, D. J., A. M. Mayes, and L. G. Griffith. 2001. Nanoscale clustering of RGD peptides at polymer surfaces using comb polymers. I. Synthesis and characterization of comb thin films. *Biomacromolecules.* 2:85-94.
- Knight, B., C. Laukaitis, N. Akhtar, N. A. Hotchin, M. Edlund, and A. F. Horwitz. 2000. Visualizing muscle cell migration in situ. *Curr. Biol.* 10:576-585.
- Kornberg, L. J., H. S. Earp, C. E. Turner, C. Prockop, and R. L. Juliano. 1991. Signal transduction by integrins: increased protein tyrosine phosphorylation caused by clustering of beta-1 integrins. *Proc. Natl. Acad. Sci. U.S.A.* 88:8392-8396.
- LaFlamme, S. E., S. K. Akiyama, and K. M. Yamada. 1992. Regulation of fibronectin receptor distribution. *J. Cell Biol.* 117:437-447.
- Lauffenburger, D. A., and A. F. Horwitz. 1996. Cell migration: a physically integrated molecular process. *Cell.* 84:359-369.
- Lauffenburger, D. A., and J. L. Linderman. 1993. Receptors: Models for Binding, Trafficking, and Signaling. Oxford University Press, New York.
- Lotz, M. M., C. A. Burdsal, H. P. Erickson, and D. R. McClay. 1989. Cell adhesion to fibronectin and tenascin: quantitative measurements of initial binding and subsequent strengthening response. *J. Cell Biol.* 109:1795-1805.
- Maheshwari, G., G. L. Brown, D. A. Lauffenburger, A. Wells, and L. G. Griffith. 2000. Cell adhesion and motility depend on nanoscale RGD clustering. *J. Cell Sci.* 113:1677-1686.
- Massia, S. P., and J. A. Hubbell. 1991. An RGD spacing of 440 nm is sufficient for integrin alpha V beta 3-mediated fibroblast spreading and 140 nm for focal contact and stress fiber formation. *J. Cell Biol.* 114:1089-1100.
- Metropolis, N., A. Rosenbluth, M. Rosenbluth, A. Teller, and E. Teller. 1953. Equations of state calculations by fast computing machines. *J. Chem. Phys.* 21:1087-1092.
- Miyamoto, S., S. K. Akiyama, and K. M. Yamada. 1995a. Synergistic roles for receptor occupancy and aggregation in integrin transmembrane function. *Science.* 267:883.
- Miyamoto, S., H. Teramoto, O. A. Coso, S. Gutkind, P. D. Burbelo, S. K. Akiyama, and K. M. Yamada. 1995b. Integrin function: molecular hierarchies of cytoskeletal and signaling molecules. *J. Cell Biol.* 131:791-805.
- Miyamoto, S., H. Teramoto, J. S. Gutkind, and K. M. Yamada. 1996. Integrins can collaborate with growth factors for phosphorylation of receptor tyrosine kinases and MAP kinase activation: roles of integrin aggregation and occupancy of receptors. *J. Cell Biol.* 135:1633-1642.
- Nomizu, M., K. Kuratomi, K. M. Malinda, S-Y. Song, K. Miyoshi, A. Otake, S. K. Powell, M. P. Hoffman, H. K. Kleinman, and Y. Yamada.

1998. Cell binding sequences in the mouse laminin  $\alpha 1$  chain. *J. Biol. Chem.* 273:32491–32499.
- Oh, E-S., A. Woods, and J. R. Couchman. 1997. Multimerization of the cytoplasmic domain of syndecan-4 is required for its ability to activate protein kinase C. *J. Biol. Chem.* 272:11805–11811.
- Pelham, R. J., and Y-L. Wang. 1997. Cell locomotion and focal adhesions are regulated by substrate flexibility. *Proc. Natl. Acad. Sci. U.S.A.* 94:13661–13665.
- Piper, J. W., R. A. Swerlick, and C. Zhu. 1998. Determining force dependence of two-dimensional receptor-ligand binding affinity by centrifugation. *Biophys. J.* 74:492–513.
- Ruoslahti, E. 1996. RGD and other recognition sequences for integrins. *Annu. Rev. Cell. Dev. Biol.* 12:697–715.
- Schmidt, C. E., A. F. Horwitz, D. A. Lauffenburger, and M. P. Sheetz. 1993. Integrin-cytoskeletal interactions in migrating fibroblasts are dynamic, asymmetric, and regulated. *J. Cell Biol.* 123:977–991.
- Segel, L. A., T. Volk, and B. Geiger. 1983. On spatial periodicity in the formation of cell adhesions to a substrate. *Cell Biophys.* 5:95–104.
- Shaw, L. M., J. M. Messier, and A. M. Mercurio. 1990. The activation-dependent adhesion of macrophages to laminin involves cytoskeletal anchoring and phosphorylation of the  $\alpha_6\beta_1$  integrin. *J. Cell Biol.* 110:2167–2174.
- Spring, J., K. Beck, and R. Chiquet-Ehrismann. 1989. Two contrary functions of tenascin: dissection of the active sites by recombinant tenascin fragments. *Cell.* 59:325–334.
- Ward, M. D., and D. A. Hammer. 1993. A theoretical analysis for the effect of focal contact formation on cell-substrate adhesion strength. *Biophys. J.* 64:936–959.
- Ward, M. D., and D. A. Hammer. 1994. Focal contact assembly through cytoskeletal polymerization: steady state analysis. *J. Math. Biol.* 32:677–704.
- Wary, K. K., A. Mariotti, C. Zurzolo, and F. G. Giancotti. 1998. A requirement for caveolin-1 and associated kinase Fyn in integrin signaling and anchorage-dependent cell growth. *Cell.* 94:625–634.
- Weber, P. C., D. H. Ohlendorf, J. J. Wendoloski, and F. R. Salemme. 1989. Structural origins of the high-affinity biotin binding to streptavidin. *Science.* 243:85–88.
- Wei, Y., X. Yang, Q. Liu, J. Wilkins, and H. Chapman. 1999. A role for caveolin and the urokinase receptor in integrin-mediated adhesion and signaling. *J. Cell Biol.* 144:1285–1294.
- Xiao, Y., and G. A. Truskey. 1996. Effect of receptor-ligand affinity on the strength of endothelial cell adhesion. *Biophys. J.* 71:2869–2884.
- Xie, H., M. A. Pallero, K. Gupta, P. Chang, M. F. Ware, W. Witke, D. J. Kwiatowski, D. A. Lauffenburger, J. E. Murphy-Ullrich, and A. Wells. 1998. EGF receptor regulation of motility: EGF induces disassembly of focal adhesions independently of the motility-associated PLC $\gamma$  signaling pathway. *J. Cell Sci.* 111:615–624.
- Yamada, K. M., S. Aota, S. K. Akiyama, and S. E. LaFlamme. 1992. Mechanisms of fibronectin and integrin function during cell adhesion and migration. *Cold Spring Harbor Symp. Quant. Biol.* 57:203–211.
- Yauch, R. L., D. P. Felsenfeld, S-K. Kraeft, L. B. Chen, M. P. Sheetz, and M. P. Hemler. 1997. Mutational evidence for control of cell adhesion through integrin diffusion/clustering, independent of ligand binding. *J. Exp. Med.* 186:1347–1355.
- Zamir, E., B-Z. Katz, S. Aota, K. Yamada, B. Geiger, and Z. Kam. 1999. Molecular diversity of cell-matrix interactions. *J. Cell Sci.* 112:1655–1669.